

RESEARCH

Open Access



A promising Ka band leaky-wave antenna based on a periodic structure of non-identical irregularities

Mohamed N. Shaaban^{1*} , Mohamed Hassan Essai Ali¹ , M. S. Yasseen¹, Aydar R. Nasybullin² and Yuri E. Sedelnikov²

*Correspondence:
eng.m.nor@azhar.edu.eg

¹ Electrical Engineering
Department, Faculty
of Engineering, Al Azhar
University, Qena, Egypt
² Kazan National Research
Technical University named
after A.N. Tupolev-KAI, Kazan,
Russia

Abstract

This paper presents a new periodic grooved dielectric leaky-wave antenna with non-identical irregularities for an extremely high-frequency range capable of performing efficiently in the Ka band through a stable gain, a decrease in the level of the side lobes, and the achievement of a narrower main lobe beam. It consists of a dielectric waveguide antenna placed inside a channelled rectangular metallic waveguide to improve performance. A dielectric rod was used to overcome the losses related to the propagation of electromagnetic waves in metal conductors. A grooved dielectric of a 21-element linear array is used to propose a simple approach for the synthesis of such antennas based on a modified energy method and is fed by a standard waveguide. It was designed and simulated at 37.2 GHz for satellite, 5G antenna, and radar applications. The major novelty of this study is the ability to control the direction of the main lobe through non-identical irregularities in geometric parameters such as the width, height, and distance between each element. Radiation techniques have been extensively studied using simulations. A performance antenna with radiation efficiency of 99.35%, gain of 22 dBi, width of radiation pattern of 3.2°, and side lobe level (SLL) of −18.3 dB has been achieved.

Keywords: Dielectric waveguides, Leaky-wave antennas, Periodic structures, Antenna arrays, Non-identical irregularities, Millimetre waveband

1 Introduction

Researchers studied the fifth generation cellular network technology (5G), and they found that it has a greater capacity while it uses a new spectrum [1–7]. 5G millimetre-wave bands use frequency bands ranging from 24–100 GHz [8–12], supporting a wide range of devices [13–16] and demonstrating the performance of outlining 5G service requirements [17, 18]. Leaky-wave antennas (LWAs) are highly promising millimetre and submillimetre wave directional antennas [19–21] due to their ability to achieve higher direct radiation [22–24] with single or multiple feedings [25, 26], resulting in a compact structure [27] with low energy consumption [28, 29]. Numerous studies have discussed the functionality of resonant cavities by using the LWA principle [30–35]. For

the first time, an antenna of this type was proposed by Oliner [36] and was called the “leaky-wave”. A typical antenna of this type is a surface waveguide with a periodic system of irregularities [37, 38]. The presence of irregularities leads to the transformation of the surface waves into radiating waves. This is reflected in the interpretation of the wave propagation coefficient as a complex quantity $\gamma = \alpha + j\beta$, the real part of which is due to radiation into the surrounding space. The imaginary part characterises the phase delay of the wave propagating in the waveguide. The flexibility of periodic type LWAs for scanning over a wide angular range is one of their advantages [39]. Filling the guiding structures with dielectric is a good approach for producing a slow-wave mode [40–43]. There are different types of open waveguide structures (dielectric rods with different cross-sectional shapes). The most common are dielectric rods with a ground plane and a dielectric rod placed in a channel metal waveguide. In addition, there are various irregularities, such as longitudinal or transverse conductor strips on the waveguide surface [44], grooves [45, 46], holes in the dielectric rod [47, 48], quarter-wave pins on the walls of the channel metal waveguide [49], and fractal antennas [50–55]. Each of the presented options for dielectric waveguide irregularities is quite simple in terms of technological implementation and has characteristic advantages and disadvantages. Metal strips are easily implemented by using printing technology with foil materials. However, there is a slight increase in thermal losses in this case. Irregularities in the form of grooves do not exhibit this disadvantage. However, their execution requires mechanical processing operations, which complicates manufacturing. The remainder of this paper is organized as follows. Section 2 presents the methodology of the current distribution of LWA array model with non-identical irregularities. The contribution and advantages of the proposed work were involved. Section 3 details the synthesis of LWAs with non-identical irregularities. A new idea is put forward for how to implement the antenna element geometry based on each component’s coupling coefficient value. Section 4 presents the simulation results and is divided into three sections. The first shows the results for an antenna with identical irregularities. The second shows results for an antenna with non-identical irregularities. The third section provides a comparison between the results of the antenna with identical and non-identical irregularities. Finally, Sect. 5 concludes the paper and summarises the radiating characteristics based on a modified energy approach and work results.

2 Methods

2.1 The model of LWA with non-identical irregularities

To achieve the LWA amplitude distribution of radiating current $|J(z)|$ (different from the exponential), the attenuation coefficient of the wave propagating along the aperture must be changed as follows: $\alpha(|X|, z) \xrightarrow{|X|} \alpha_{\text{given}}(z, |J_{\text{given}}(z)|)$. ($|X|$ -parameters of waveguide and irregularities, z -coordinate along the antenna axis). The implementation of this principle requires the presence of data about the quantitative dependence of the attenuation coefficient $\alpha(z)$ in a longitudinally inhomogeneous dielectric waveguide on the parameters of the waveguide and irregularities [56, 57]. A solution to a specified task is difficult. The use of numerical electromagnetic modelling (CST, HFSS, etc.) to determine the parameters of irregularities based on a given $\alpha_{\text{given}}(z, |J_{\text{given}}(z)|)$ is difficult due to the need to organize a large number of options that differ in waveguide size, irregularities,

and interelement distance. Therefore, it is necessary to develop simple engineering procedures for the synthesis of irregularities in longitudinally inhomogeneous waveguides using a given amplitude-phase distribution of radiating currents in an antenna aperture. These can be used to obtain the first approximation when designing such antennas and refer to the methods of local optimization. This technique can be developed during the transition to an antenna model as a linear antenna array [58]. According to the indicated model, the antenna is considered an antenna array with serial excitation. The energy approach is widely used for the approximate calculation of linear radiating systems in the form of a periodic system of identical radiators with a sequential excitation scheme [57]. In [59], a modified energy approach was proposed and approved, which summarises the approach for the case of an almost periodic system of non-identical radiators. According to the specified approach, a dielectric waveguide with irregularities is represented by an antenna array model with a serial excitation of its elements. The antenna array model is shown in Fig. 1a. A section of a waveguide with irregularity is considered an element of the array. The coordinates of the radiators correspond to the centers of the sections. The interaction of the waveguide mode with the radiators is characterised by the power-coupling coefficient. Figure 1b shows the mechanism of antenna element excitation. According to the energy approach in the antenna, with sequential excitation the amplitude-phase radiating current distribution of the antenna array model can be represented as:

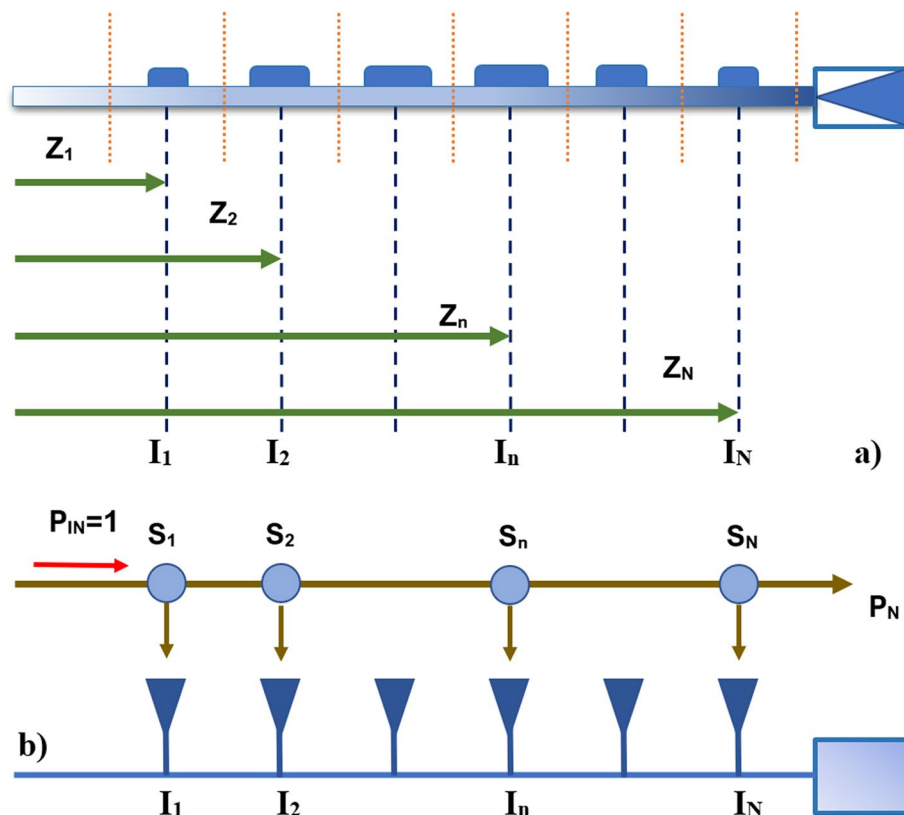


Fig. 1 Antenna array model: **a** current distribution of the antenna array model; **b** The power coupling coefficients of the k -th array element

$$|I_n| = \sqrt{s_n \prod_{k=1}^{n-1} (1 - s_k)} \quad (1)$$

$$\arg(I_n) = \sum_{k=1}^{n-1} \beta_k d_k \quad (2)$$

where s_k is the power coupling coefficient of the k -th array element (relative power fraction of the undergoing wave radiated by the n -th element) and β_k is the wave-number in the waveguide part from $k-1$ to the k -th element.

2.2 The contributing advantages of the proposed work are as follows:

(1) The design uses a periodic structure of a dielectric waveguide with non-identical irregular grooves in a dielectric rectangular rod, which are placed inside the channelled waveguide. One of the disadvantages of LWAs with identical irregularities is the relatively high level of side lobes ($-10 \dots -12$ dB). However, the disadvantage is the exponential distribution of the radiating equivalent current in the antenna. The use of non-identical irregularities allows for a change in the distribution of the current and a reduction in the level of the side lobes. (2) The non-identical irregularities methodology allows us to correct the phase velocity in a dielectric waveguide. This study proposes a simple and effective method for synthesizing the parameters of irregularities depending on the required form of the current distribution.

3 LWA synthesis

The LWA under consideration consists of a dielectric rectangular rod with irregularities in the form of grooves and a channel metal waveguide (Fig. 2). Serial excitation of the antenna through the section of a rectangular waveguide with a transition horn was used.

The calculation of the antenna radiation pattern is performed using classical relations, where the amplitude-phase distribution $I_n = |I_n|e^{j\arg(I_n)}$ is in accordance with (1)–(2) and the coordinates of the radiators (Fig. 1):

$$F(\theta) = \sum_{n=1}^N g_n(\theta) |I_n| e^{j\arg(I_n)} e^{-2j\pi z_n(\sin(\theta)/\lambda)} \quad (3)$$

where $g_n(\theta)$ represents the n -th radiator's radiation pattern. The n -th section of the waveguide exhibited irregularity. Radiation pattern $g_n(\theta)$ can be considered equal to

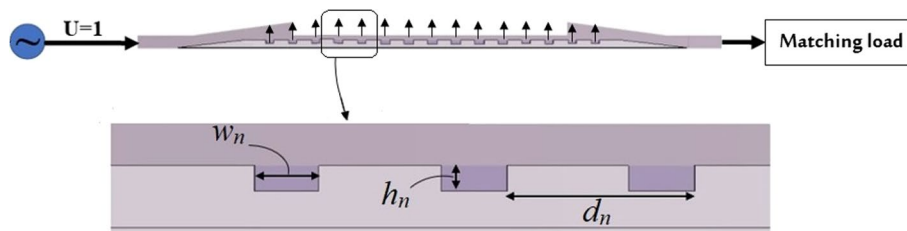


Fig. 2 A dielectric waveguide with non-identical irregularities

$g_n(\theta) \approx g(\theta)$ because the electrical dimensions of the sections are almost the same. Then:

$$F(\theta) = g(\theta) \sum_{n=1}^N |I_n| e^{j \arg(I_n)} e^{-2j\pi z_n (\sin(\theta)/\lambda)} \quad (4)$$

The efficiency coefficient and antenna aperture efficiency are:

$$\text{Efficiency} = 1 - \prod_{k=1}^N (1 - s_k) \quad (5)$$

$$\text{Antenna Aperture Efficiency} = \frac{\left| \sum_1^N I_n^2 \right|}{N \sum_1^N |I_n|^2} \quad (6)$$

Relations (1)–(6) can be used to solve the analysis problem (looking for radiation pattern and other basic parameters) and the synthesis problem (looking for geometric parameters) using a given radiation pattern or other criteria. Let us consider an antenna in the form of a dielectric waveguide with non-identical irregularities in the channel of a metallic waveguide, connected to a matching load. For the given waveguide parameters and irregularities, the amplitude-phase distribution for the antenna array model is determined by the relations (1)–(2). The objective of antenna array synthesis is to determine the parameters of the irregularities and their locations according to the predetermined amplitude-phase distribution in the antenna aperture. In the case of travelling wave antennas, the specified distribution is in-phase (or linear for inclined radiation). We restricted ourselves to the case of transverse radiation obtained with a given beam width and side-lobe level. Under these conditions, the specified in-phase distribution of the phase and amplitude distributions can be considered as a function of $J_{n(\text{given})} = |I_n|$. The form of $J_{n(\text{given})}$ and the electrical length of the antenna L_{ant} are determined according to the classical aperture theory of antennas. The number of radiators is $N = L_{\text{ant}}/\lambda_{\text{waveguide}}$. The value of $\lambda_{\text{waveguide}}$ by the first approximation is determined by the specified dimensions and the parameters of the unloaded (without grooves) waveguide. The solution of the synthesis problem (looking for the irregularity parameters) is carried out in two stages, each of which is submitted in a closed form.

Stage 1: Let the specified distribution be normalised in such a way that:

$$\sum_{n=1}^N J_n^2 = 1 \quad (7)$$

From relationship (1) directly follows:

$$s_1 = C_{\text{Norm}} J_1^2 \quad (8)$$

$$s_2 = C_{\text{Norm}} J_1^2 / 1 - s_1 \quad (9)$$

$$s_n = C_{\text{Norm}} J_n^2 / \prod_{k=1}^{n-1} (1 - s_k) \quad (10)$$

In relationships (8)–(10), the normalising multiplier $C_{\text{Norm}} < 1$ is selected such that all the found coupling coefficients do not exceed the maximum possible value s_{max} for this type and size of waveguide.

$$\begin{cases} C_{\text{Norm}} \rightarrow \max \\ \text{When } s_n(C_{\text{Norm}}) < s_{\text{max}}, n = 1 \dots N \end{cases} \quad (11)$$

The dimensions of the w_n and h_n irregularities are determined using the inverse of function $s(w, h)$ based on the discovered s_n .

Stage 2: After determining the irregularity parameters, the coordinates of the radiators were adjusted. The requirement is determined as follows. The initial geometry of the lattice is an equidistant system with a step equal to the wavelength of the waveguide (unloaded). The presence of irregularities leads to a change in the phase velocity of the waves in the waveguide. The phase distribution changes accordingly, which ceases to be in-phase. The coordinates of the radiators should be slightly changed to restore the in-phase distribution in the aperture. We assume that in the neighbourhood of the n -th irregularity, the value of the phase coefficient is equal to:

$$\beta_n = \beta(w_n, h_n) \quad (12)$$

Knowing the dependency of the wave phase velocity on the parameters of irregularities, the correction of the coordinates of the radiators is performed such that the distance between the n -th and $n+1$ radiators is equal to the local wavelength value in the loaded waveguide.

$$z_{n+1} - z_n = \frac{2\pi}{\beta_n} = \lambda_{\text{waveguide}}(w_n, h_n) \quad (13)$$

The modified energy approach is distinguished by the algorithm for determining the relationships $s(w, d)$ and $\lambda_{\text{waveguide}}(w, h)$ [57]. The algorithm is based on the numerical calculation of the S_{21} coefficient of the channel waveguide with the LWA and antenna radiation pattern using electromagnetic simulation software. In this case, the LWA model was a periodic dielectric waveguide with identical irregularities. Consequently, for different combinations of specified values of w and d , we determine the absolute values $|S_{21}|$ that are used to determine the relationship for the coupling coefficient:

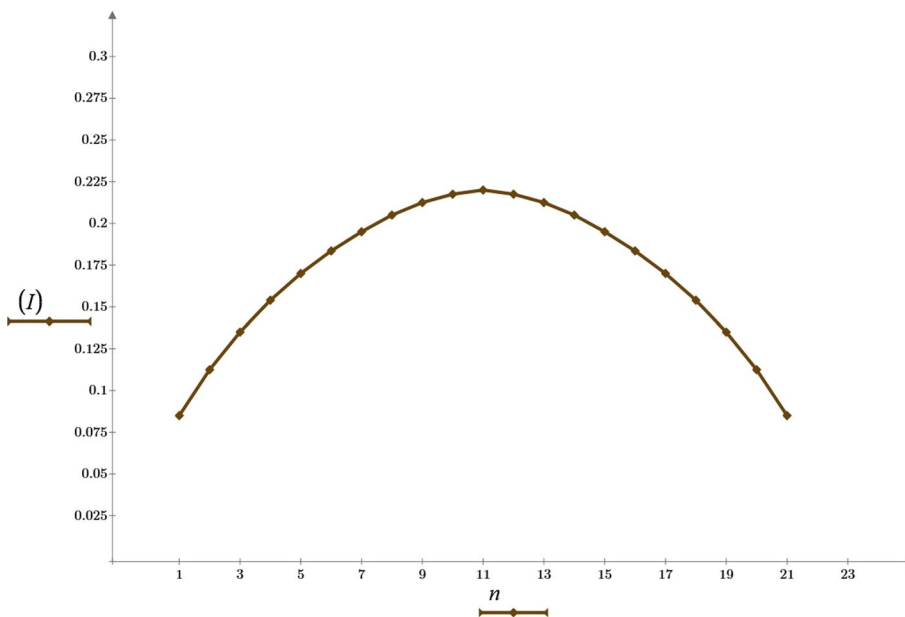
$$s(w, h) = \frac{1 - |S_{21}|^2}{N} \quad (14)$$

The radiation pattern was used to determine the $\lambda_{\text{waveguide}}(w, h)$ function. The angular position $\theta_{\text{max}}(w, h)$ of its maximum is determined, and the value of is

$$\lambda_{\text{waveguide}}(w, h) = \left(\sin(\theta_{\text{max}}(w, h)) + \frac{\lambda_0}{d} \right) \lambda_0 \quad (15)$$

Table 1 Given amplitude distribution for $N = 21$ transversely radiating antenna

I_n	Value	I_n	Value	I_n	Value
I_1	0.085	I_8	0.205	I_{15}	0.195
I_2	0.1125	I_9	0.2125	I_{16}	0.1835
I_3	0.135	I_{10}	0.2175	I_{17}	0.17
I_4	0.154	I_{11}	0.22	I_{18}	0.154
I_5	0.17	I_{12}	0.2175	I_{19}	0.135
I_6	0.1835	I_{13}	0.2125	I_{20}	0.1125
I_7	0.195	I_{14}	0.205	I_{21}	0.085

**Fig. 3** A predetermined amplitude distribution

Now, we present the results of the of the transversely radiating antenna with $N = 21$ (as shown in Table 1 and Fig. 3 with the given amplitude distribution).

Table 2 lists the calculated values of the coupling coefficients, and Fig. 4 shows them in a graph.

The calculated local values of the wavelength $\lambda_{\text{waveguide}}(w_n, h_n)$ in a loaded waveguide, where w_n and h_n are the dimensions of irregularities listed in Table 3.

The data below are the results of the electrodynamic modelling of the antenna performed on the basis of a groove dielectric waveguide. The dimensions of the groove correspond to the standard metal waveguide with a cross section of 7.2×3.6 mm, dielectric-Teflon, 2 mm thick. The excitation is carried out by a standard waveguide using the transition shown in Fig. 5.

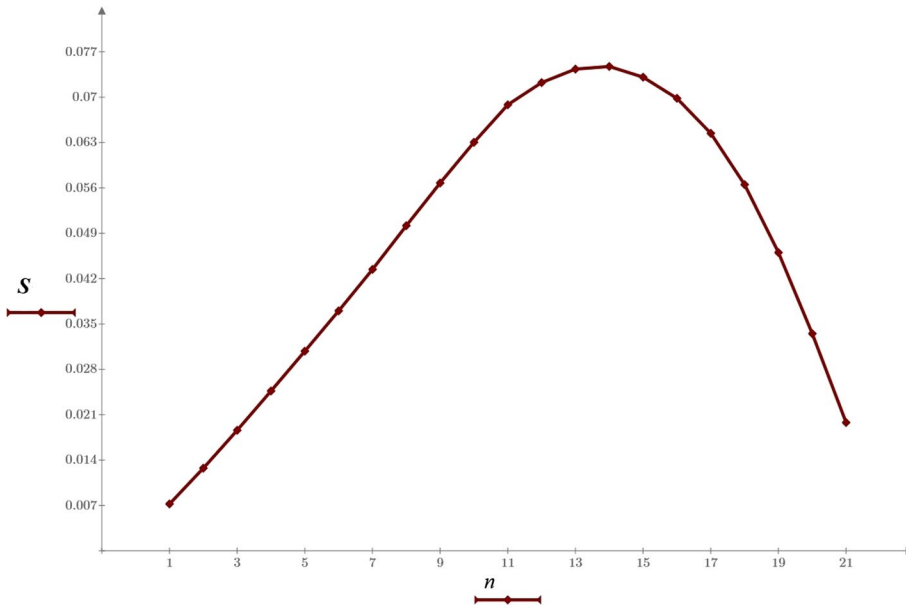
4 Results and discussion

4.1 Antenna results with identical irregularities

We should start with the results of identical irregularities and, after showing the performance parameter, make a comparison with the new results of non-identical

Table 2 The values of distances d_n and coupling coefficients s_n corresponding to design geometry

d_n	Value	d_n	Value	s_n	Value	s_n	Value
d_1	6.8	d_{12}	83.3065	s_1	0.00723	s_{12}	0.07226
d_2	13.609	d_{13}	90.3365	s_2	0.01275	s_{13}	0.07435
d_3	20.391	d_{14}	97.3665	s_3	0.01859	s_{14}	0.07475
d_4	27.1975	d_{15}	104.3965	s_4	0.02466	s_{15}	0.0731
d_5	34.0975	d_{16}	111.4235	s_5	0.0308	s_{16}	0.06983
d_6	41.0565	d_{17}	118.4635	s_6	0.03703	s_{17}	0.06444
d_7	48.0565	d_{18}	125.4635	s_7	0.04343	s_{18}	0.05652
d_8	55.0565	d_{19}	132.4693	s_8	0.05017	s_{19}	0.04604
d_9	62.0565	d_{20}	139.4193	s_9	0.05676	s_{20}	0.03351
d_{10}	69.1065	d_{21}	146.1793	s_{10}	0.06304	s_{21}	0.01979
d_{11}	76.2065			s_{11}	0.06884		

**Fig. 4** Antenna coupling coefficients

irregularities. The design provides S_{11} and a radiation pattern as shown in Figs. 6, 7 and 8. S_{11} equals -14.97 dB at frequency 37.2 GHz.

As shown at Figs. 7 and 8, the calculated radiation pattern at frequency $F = 37.2$ GHz is 20.9 dBi, width of radiation pattern is 2.8° , and the side lobe equals -10.5 dB.

4.2 Antenna results with non-identical irregularities

Now the proposed design provides good performance parameters as shown at Figs. 9, 10 and 11. S_{11} equals -16.04 dB at frequency 37.2 GHz. As shown in Fig. 9, the calculated radiation pattern at frequency $F = 37.2$ GHz is 22 dBi, the width of the radiation pattern is 3.2° , and the side lobe equals -18.3 dB.

Table 3 The dimensions of irregularities w_n and h_n , and the calculated local values of the wavelength $\lambda_{\text{waveguide}}(w_n, h_n)$ for individual radiating element

w_n	Value	h_n	Value	$\lambda_{\text{waveguide}}$	Value
w_1	1.1	h_1	1.0853	λ_1	6.8
w_2	1.259	h_2	0.8946	λ_2	6.809
w_3	1.402	h_3	1.0285	λ_3	6.782
w_4	1.831	h_4	0.965	λ_4	6.8065
w_5	2	h_5	0.9135	λ_5	6.9
w_6	2.26	h_6	1.0396	λ_6	6.959
w_7	2.4	h_7	1.0044	λ_7	7
w_8	2.75	h_8	1.0747	λ_8	7
w_9	2.9	h_9	1.01	λ_9	7
w_{10}	3.05	h_{10}	1.0035	λ_{10}	7.05
w_{11}	3.1	h_{11}	1.0507	λ_{11}	7.1
w_{12}	3.1	h_{12}	1.0573	λ_{12}	7.1
w_{13}	3.1	h_{13}	0.9962	λ_{13}	7.03
w_{14}	3.1	h_{14}	0.9976	λ_{14}	7.03
w_{15}	3.1	h_{15}	0.9937	λ_{15}	7.03
w_{16}	3	h_{16}	1.0203	λ_{16}	7.027
w_{17}	3	h_{17}	1.0186	λ_{17}	7.04
w_{18}	2.9	h_{18}	1.009	λ_{18}	7
w_{19}	2.402	h_{19}	1.0171	λ_{19}	7.0058
w_{20}	2.25	h_{20}	1.026	λ_{20}	6.95
w_{21}	1.4	h_{21}	0.9928	λ_{21}	6.76

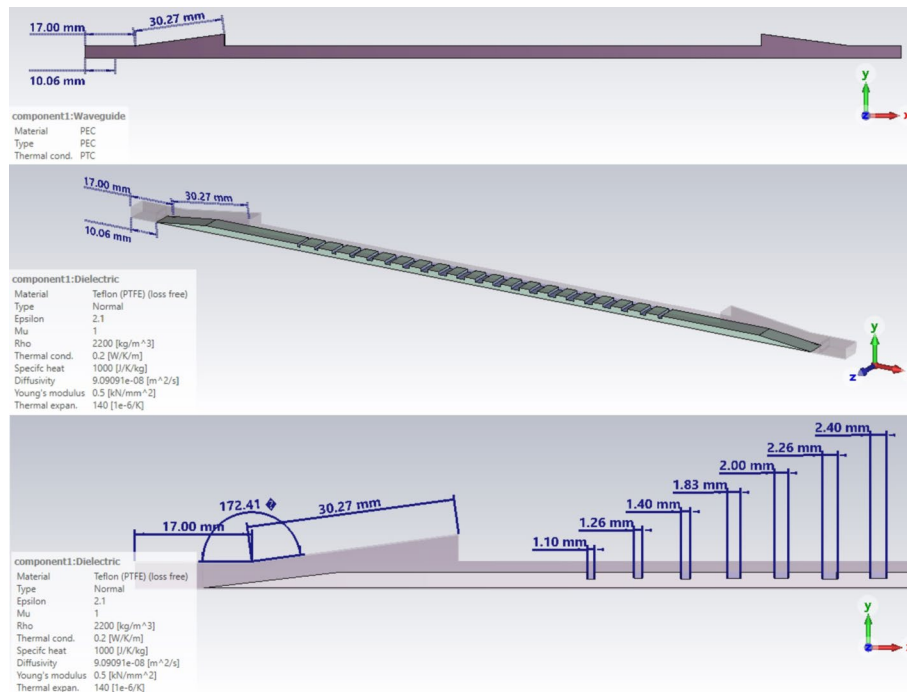


Fig. 5 Antenna simulation model (geometry with one-sided excitement, number of elements 21, dimensions of waveguide 7.2×3.6 mm)

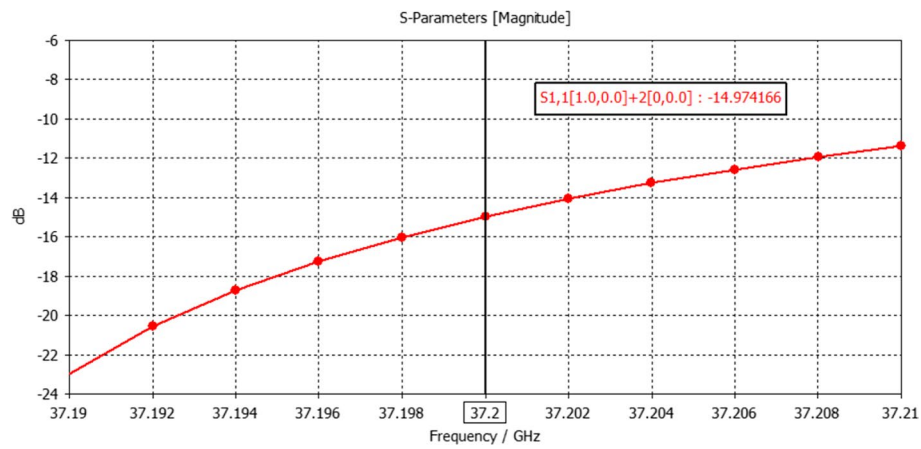


Fig. 6 S_{11} at frequency $F = 37.2$ GHz for antenna with identical irregularities

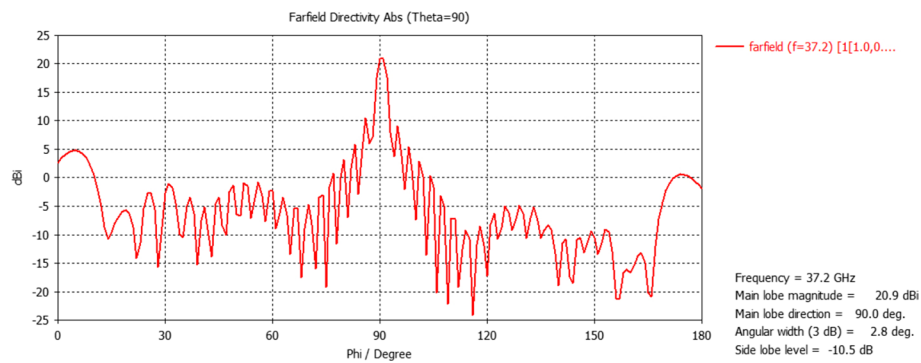


Fig. 7 1-D radiation pattern at frequency $F = 37.2$ GHz for antenna with identical irregularities

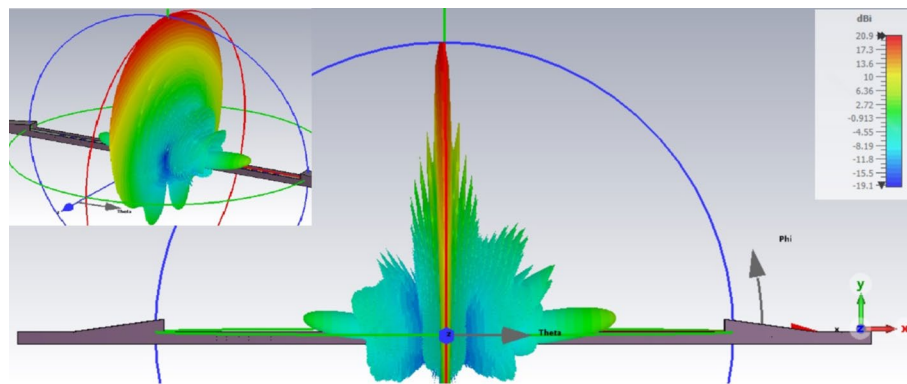


Fig. 8 3D radiation pattern at frequency $F = 37.2$ GHz (RP: 20.9 dBi, width of RP: 2.8°, side lobe: -10.5 dB) for antenna with identical irregularities

Figures 10 and 11 show 1D and 3D radiation patterns according to the predetermined amplitude distribution (Fig. 3) calculated by electromagnetic numerical modelling in the CST. Figure 12 shows a comparison between the results obtained by

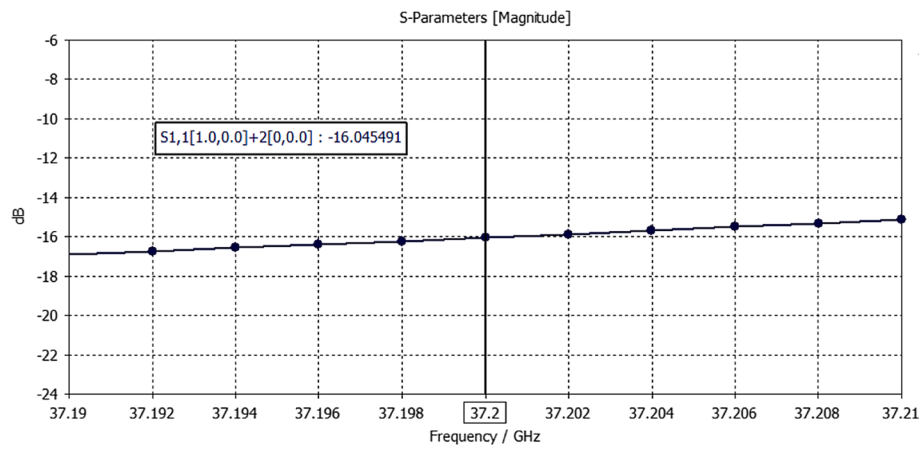


Fig. 9 S11 at frequency $F = 37.2$ GHz for antenna with non-identical irregularities

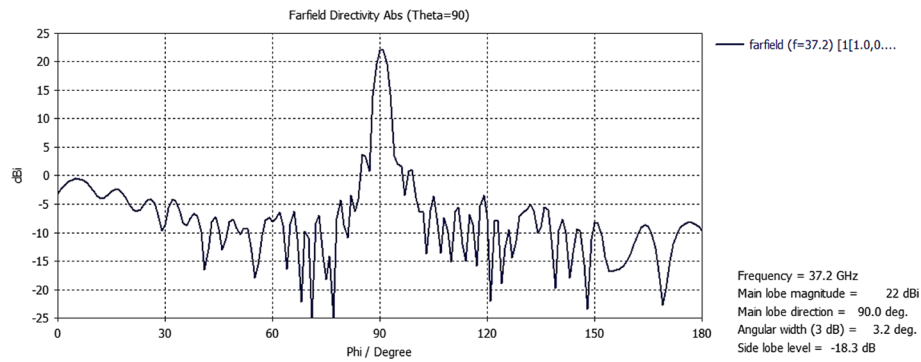


Fig. 10 1-D radiation pattern at frequency $F = 37.2$ GHz for antenna with non-identical irregularities

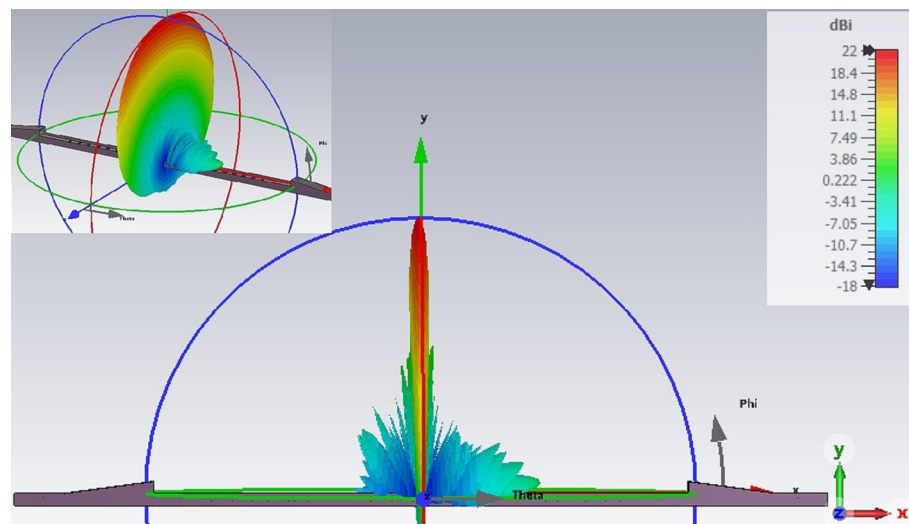


Fig. 11 3D radiation pattern at frequency $F = 37.2$ GHz (RP: 22 dBi, width of RP: 3.2°, Side lobe: -18.3 dB) for antenna with non-identical irregularities

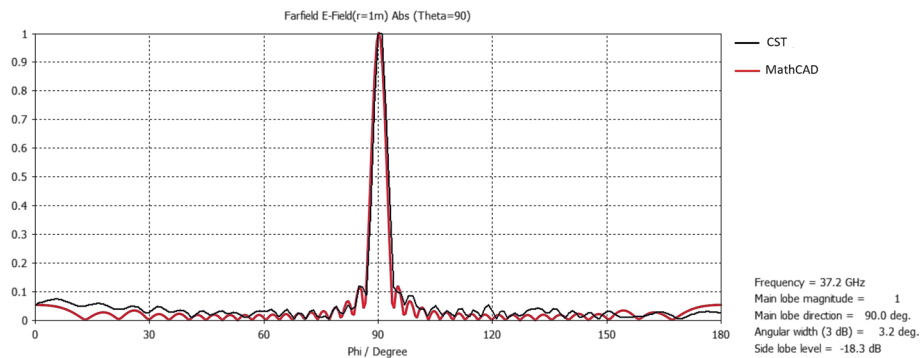


Fig. 12 Comparison of radiation patterns for antenna with non-identical irregularities obtained by numerical electromagnetic calculation and modified energy approach

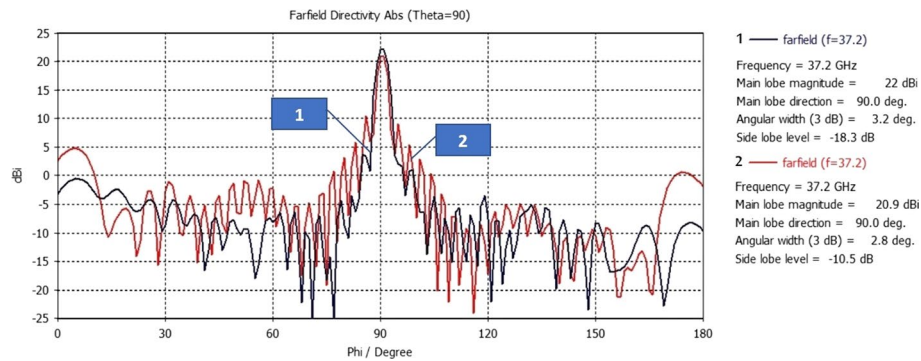


Fig. 13 Comparison of the 1-D calculated radiation pattern at frequency $F = 37.2$ GHz for antenna with identical and non-identical irregularities

numerical simulation in CST (black line) and a modified energy approach (purple line). It can be seen that the similarity is very close, especially in the area of the main lobe. The efficiency of the considered antenna was 83.6%.

4.3 A comparison of the results of antennas with identical and non-identical irregularities

Figures 13 and 14 show comparisons of radiation patterns and S_{11} coefficients for antennas with identical and non-identical irregularities.

An antenna with non-identical irregularities has a better side lobe level (7.8 dB better) with almost identical gain and an absolute value of S_{11} . Only a slight increase in radiation pattern width (0.4°) is observed. Table 4 shows a comparison between the proposed work and previous works. The proposed antenna exhibits superior characteristics at mm-wave frequency bands, including low SLL with high efficiency and gain.

5 Conclusions

Antennas of the “leaky-wave” type, based on dielectric waveguide structures, are a promising class of flat antennas in the EHF band. The approach proposed in the work and synthesis of such structures is based on antenna representation as an almost periodic

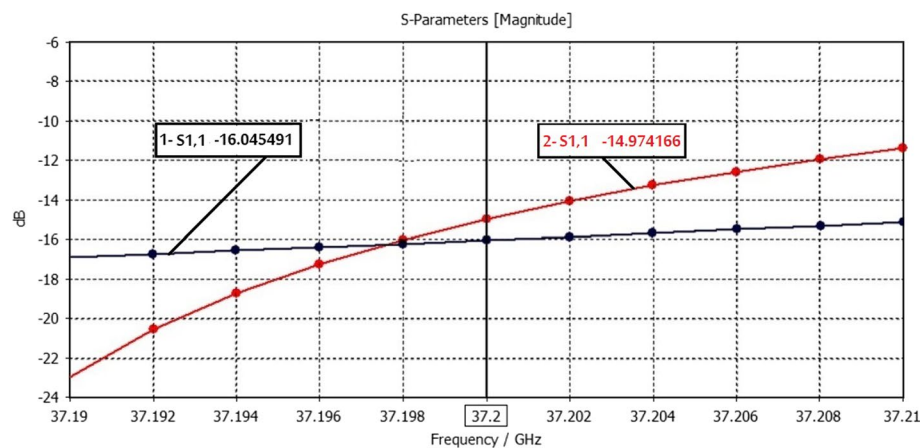


Fig. 14 Comparison of the S11 at the same frequency $F = 37.2$ GHz for antenna with identical and non-identical irregularities

Table 4 Performance comparison of the presented waveguide arrays

References	Frequency (GHz)	Gain (dBi)	SLL (dB)	Rad. eff.(%)
[60]	32	16.1	− 13.0	83
[61]	30.2	27.0	− 13.0	80
[62]	30	15.5	− 10.0	87
[63]	37.5	18.0	12.6	N/A
This work	37.2	22.0	− 18.3	99.35

antenna array with a preliminary analysis of radiating characteristics based on a modified energy approach. The analysis showed the validity of the proposed approach, which ensured acceptable coordination of the calculated data and was obtained using modern means of electromagnetic modeling. In this study, we developed a combination of technical solutions to improve the technical indicators of antennas fabricated using dielectric waveguides. The solution to the task includes the following components: First, the development of the synthesis method of a linear antenna array model of LWA with non-identical irregularities Second, analysis of an antenna containing irregularities in the form of grooves in a dielectric.

Abbreviations

LWA	Leaky-wave antenna
EHF	Extremely high-frequency
SLL	Side lobe level
5G	Fifth generation cellular network technology
CST	Computer simulation technology
HFSS	High-frequency structure simulator
RP	Radiation pattern

Acknowledgments

Not applicable.

Authors contributions

Dr. MNS and Prof. YES contributed to conceptualization; Dr. MNS, Assoc. Prof. MHEA and Dr. MSY were involved in formal analysis and funding acquisition; Dr. MNS and Dr. ARN contributed to investigation and writing-original draft, and provided resources and software; Prof. YES was involved in methodology; Dr. MNS, Prof. YES and Assoc. Prof. MHEA contributed to project administration, supervision, and writing-review editing. All authors read and approved the final manuscript.

Funding

Open access funding provided by The Science, Technology & Innovation Funding Authority (STDF) in cooperation with The Egyptian Knowledge Bank (EKB).

Availability of data and materials

Not applicable.

Declarations**Consent for publication**

All authors have agreed and given their consent for submission of this paper to EURASIP Journal of Wireless Communications and Networking.

Competing interests

The authors declare that they have no competing interests.

Received: 11 July 2022 Accepted: 19 September 2022

Published online: 01 October 2022

References

1. M. Khalid, S. Iffat Naqvi, N. Hussain, M. Rahman, S.S. Mirjavadi, M.J. Khan, Y. Amin, 4-port mimo antenna with defected ground structure for 5g millimeter wave applications. *Electronics* **9**(1), 71 (2020)
2. Z. Liu, X. Cheng, Y. Yao, T. Yu, J. Yu, X. Chen, Broadband transition from rectangular waveguide to groove gap waveguide for mm-wave contactless connections. *Electronics* **9**(11), 1820 (2020)
3. U. Gustavsson, P. Frenger, C. Fager, T. Eriksson, H. Zirath, F. Dielacher, C. Studer, A. Pärssinen, R. Correia, J.N. Matos et al., Implementation challenges and opportunities in beyond-5g and 6g communication. *IEEE J. Microw.* **1**(1), 86–100 (2021)
4. R.K. Saha, An overview and mechanism for the coexistence of 5g nr-u (new radio unlicensed) in the millimeter-wave spectrum for indoor small cells. *Wirel. Commun. Mobile Comput.* **2021** (2021)
5. V.Y.K. Loung et al., Capacity estimation for 5g cellular networks. *Turk. J. Comput. Math. Educ. (TURCOMAT)* **12**(3), 4530–4537 (2021)
6. X. Lin, N. Lee, *5G and Beyond* (Springer, Berlin, 2021)
7. S. Jayakumar et al., A review on resource allocation techniques in d2d communication for 5g and b5g technology. *Peer-to-Peer Netw. Appl.* **14**(1), 243–269 (2021)
8. J.W. Frank, Electromagnetic fields, 5g and health: what about the precautionary principle? *J. Epidemiol. Community Health* **75**(6), 562–566 (2021)
9. V. Kazachkov, N. Soldatenkova, Bit error rate performance of power domain non-orthogonal multiple access systems, in: 2021 Systems of Signals Generating and Processing in the Field of on Board Communications, pp. 1–5 (2021). IEEE
10. A.-E.M. Taha, Quality of experience in 6g networks: outlook and challenges. *J. Sens. Actuator Netw.* **10**(1), 11 (2021)
11. C. Han, Y. Wang, Y. Li, Y. Chen, N.A. Abbasi, T. Kürner, A.F. Molisch, Terahertz wireless channels: a holistic survey on measurement, modeling, and analysis. *IEEE Commun. Surv. Tutorials* (2022)
12. J. Parikh, A. Basu, Technologies assisting the paradigm shift from 4g to 5g. *Wirel. Pers. Commun.* **112**(1), 481–502 (2020)
13. N. Gupta, S. Sharma, P.K. Juneja, U. Garg, Sdnfv 5g-iot: A framework for the next generation 5g enabled iot, in: 2020 International Conference on Advances in Computing, Communication & Materials (ICACCM), pp. 289–294 (2020). IEEE
14. A.A. Salih, S. Zeebaree, A.S. Abdurhaheem, R.R. Zebari, M. Sadeeq, O.M. Ahmed, Evolution of mobile wireless communication to 5g revolution. *Tech. Rep. Kansai Univ.* **62**(5), 2139–2151 (2020)
15. S. Jayakumar et al., A review on resource allocation techniques in d2d communication for 5g and b5g technology. *Peer-to-Peer Netw. Appl.* **14**(1), 243–269 (2021)
16. S. Sharma, P. Agarwal, S. Mohan, Security challenges and future aspects of fifth generation vehicular adhoc networking (5g-vanet) in connected vehicles. in: 2020 3rd International Conference on Intelligent Sustainable Systems (ICISS), pp. 1376–1380 (2020). IEEE
17. R. Dong, C. She, W. Hardjawana, Y. Li, B. Vucetic, Deep learning for radio resource allocation with diverse quality-of-service requirements in 5g. *IEEE Trans. Wireless Commun.* **20**(4), 2309–2324 (2020)
18. X. Li, A. Garcia-Saavedra, X. Costa-Perez, C.J. Bernardos, C. Guimarães, K. Antevski, J. Mangués-Bafalluy, J. Baranda, E. Zeydan, D. Corujo et al., 5growth: An end-to-end service platform for automated deployment and management of vertical services over 5g networks. *IEEE Commun. Mag.* **59**(3), 84–90 (2021)
19. L. Wang, J.L. Gomez-Tornero, E. Rajo-Iglesias, O. Quevedo-Teruel, Low-dispersive leaky-wave antenna integrated in groove gap waveguide technology. *IEEE Trans. Antennas Propag.* **66**(11), 5727–5736 (2018)
20. M. Peter, A. Hildebrandt, C. Schlickriede, K. Gharib, T. Zentgraf, J. Forstner, S. Linden, Directional emission from dielectric leaky-wave nanoantennas. *Nano Lett.* **17**(7), 4178–4183 (2017)
21. R. Tchema, N.C. Papanicolaou, A.C. Polycarpou, An investigation of the dynamic beam-steering capability of a liquid-crystal-enabled leaky-wave antenna designed for 5g applications. *Appl. Phys. Lett.* **119**(3), 034104 (2021)
22. S.K. Patel, V. Sorathiya, T. Guo, C. Argyropoulos, Graphene-based directive optical leaky wave antenna. *Microw. Opt. Technol. Lett.* **61**(1), 153–157 (2019)

23. O. Zetterstrom, E. Pucci, P. Padilla, L. Wang, O. Quevedo-Teruel, Low-dispersive leaky-wave antennas for mmwave point-to-point high-throughput communications. *IEEE Trans. Antennas Propag.* **68**(3), 1322–1331 (2019)
24. P. Ahir, S.K. Patel, J. Parmar, D. Katrodiya, Directive and tunable graphene based optical leaky wave radiating structure. *Mater. Res. Exp.* **6**(5), 055607 (2019)
25. Y. Ma, J. Wang, Z. Li, Y. Li, M. Chen, Z. Zhang, Planar annular leaky-wave antenna array with conical beam. *IEEE Trans. Antennas Propag.* **68**(7), 5405–5414 (2020)
26. C. Hammes, A.R. Diebold, Periodic high-sensitive beam-steering leaky-wave antenna with circular polarization. *IEEE Trans. Antennas Propag.* **68**(3), 1937–1944 (2019)
27. Y. Geng, J. Wang, Y. Li, Z. Li, M. Chen, Z. Zhang, Leaky-wave antenna array with a power-recycling feeding network for radiation efficiency improvement. *IEEE Trans. Antennas Propag.* **65**(5), 2689–2694 (2017)
28. N. Javanbakht, R.E. Amaya, J. Shaker, B. Syrett, Side-lobe level reduction of half-mode substrate integrated waveguide leaky-wave antenna. *IEEE Trans. Antennas Propag.* **69**(6), 3572–3577 (2020)
29. Q. Chen, O. Zetterstrom, E. Pucci, A. Palomares-Caballero, P. Padilla, O. Quevedo-Teruel, Glide-symmetric holey leaky-wave antenna with low dispersion for 60 ghz point-to-point communications. *IEEE Trans. Antennas Propag.* **68**(3), 1925–1936 (2019)
30. A. Goudarzi, M.M. Honari, R. Mirzavand, Resonant cavity antennas for 5g communication systems: A review. *Electronics* **9**(7), 1080 (2020)
31. S. Sengupta, D.R. Jackson, A.T. Almutawa, H. Kazemi, F. Capolino, S.A. Long, Radiation properties of a 2-d periodic leaky-wave antenna. *IEEE Trans. Antennas Propag.* **67**(6), 3560–3573 (2019)
32. M.S. Rabbani, J. Churm, A. Feresidis, 60ghz-band leaky-wave antenna for remote health monitoring. in: 2019 13th European Conference on Antennas and Propagation (EuCAP), pp. 1–4 (2019). IEEE
33. C.P. Wiederhold, D.L. Sounas, A. Alù, Nonreciprocal acoustic propagation and leaky-wave radiation in a waveguide with flow. *J. Acoust. Soc. Am.* **146**(1), 802–809 (2019)
34. D. Kampouridou, A. Feresidis, Full-wave leaky-wave analysis of 1-d periodic corrugated metal surface antennas. *IEEE Antennas Wirel. Propag. Lett.* **20**(5), 863–867 (2021)
35. N.N. Elkin, A.P. Napartovich, D.V. Vysotsky, C. Sigler, C.A. Boyle, J.D. Kirch, T. Earles, D. Botez, L.J. Mawst, A. Belyanin, Analysis of mode competition in resonant leaky-wave coupled phase-locked arrays of mid-ir quantum cascade lasers. *IEEE J. Quantum Electron.* **55**(3), 1–10 (2019)
36. T. Tamir, A. Oliner, Guided complex waves, part 2: Relation to radiation patterns. in: Proceedings of the Institution of Electrical Engineers, vol. 110, pp. 325–334 (1963). IET
37. Y. Arellano, A. Hunt, O.C. Haas, Evaluation of near-field electromagnetic shielding effectiveness at low frequencies. *IEEE Sens. J.* **19**(1), 121–128 (2018)
38. T.G. Rappoport, I. Epstein, F.H. Koppens, N.M. Peres, Understanding the electromagnetic response of graphene/metallic nanostructures hybrids of different dimensionality. *ACS Photonics* **7**(8), 2302–2308 (2020)
39. M.N.M. Kehn, C.-Z. Chen, Analysis of leaky-wave radiation from corrugated parallel-plate waveguides with steerable beams by rotatable corrugations. *IEEE Trans. Antennas Propag.* **69**(9), 5455–5468 (2021)
40. A. Hasanbeigi, A. Ashrafi, H. Mehdian, Enhancement of intensity in a periodically layered metal-dielectric waveguide with magnetized plasma. *Phys. Plasmas* **24**(7), 073103 (2017)
41. Z. Sipus, M. Bosiljevac, Modeling of glide-symmetric dielectric structures. *Symmetry* **11**(6), 805 (2019)
42. A.N. Starodoumov, *Advanced Optical Instruments and Techniques* (CRC Press, Boca Raton, 2017)
43. I.Y. Lvovich, A. Preobrazhenskiy, O. Choporov, Simulation of two-dimensional periodic perfectly conducting diffraction grating with the dielectric layer. in: 2017 International Conference on Industrial Engineering, Applications and Manufacturing (ICIEAM), pp. 1–4 (2017). IEEE
44. Y. Lin, T.X. Hoang, H.-S. Chu, C.A. Nijhuis, Directional launching of surface plasmon polaritons by electrically driven aperiodic groove array reflectors. *Nanophotonics* **10**(3), 1145–1154 (2021)
45. J. Huang, S.J. Chen, Z. Xue, W. Withayachumnankul, C. Fumeaux, Wideband circularly polarized 3-d printed dielectric rod antenna. *IEEE Trans. Antennas Propag.* **68**(2), 745–753 (2019)
46. Y. Zhang, S. Lin, B. Zhu, J. Cui, Y. Mao, J. Jiao, A. Denisov, Broadband and high gain dielectric-rod end-fire antenna fed by a tapered ridge waveguide for k/ka bands applications. *IET Microw. Antennas Propag.* **14**(8), 743–751 (2020)
47. R.A.S.D. Koala, D. Headland, Y. Yamagami, F. Masayuki, T. Nagatsuma, Broadband terahertz dielectric rod antenna array with integrated half-maxwell fisheye lens. in: 2020 International Topical Meeting on Microwave Photonics (MWP), pp. 54–57 (2020). IEEE
48. J. Kulkarni, A.G. Alharbi, A. Desai, C.-Y.-D. Sim, A. Poddar, Design and analysis of wideband flexible self-isolating mimo antennas for sub-6 ghz 5g and wlan smartphone terminals. *Electronics* **10**(23), 3031 (2021)
49. M. Simone, A. Fanti, M.B. Lodi, T. Pisanu, G. Mazzarella, An in-line coaxial-to-waveguide transition for q-band single-feed-per-beam antenna systems. *Appl. Sci.* **11**(6), 2524 (2021)
50. K.C. Hwang, A modified sierpinski fractal antenna for multiband application. *IEEE Antennas Wirel. Propag. Lett.* **6**, 357–360 (2007)
51. E. Guariglia, Harmonic sierpinski gasket and applications. *Entropy* **20**(9), 714 (2018)
52. C. Puente-Baliarda, J. Romeu, R. Pous, A. Cardama, On the behavior of the sierpinski multiband fractal antenna. *IEEE Trans. Antennas Propag.* **46**(4), 517–524 (1998)
53. J. Anguera, C. Borja, C. Puente, Microstrip fractal-shaped antennas: a review. in: The Second European Conference on Antennas and Propagation, EuCAP 2007, pp. 1–7 (2007). IET
54. E. Guariglia, Entropy and fractal antennas. *Entropy* **18**(3), 84 (2016)
55. E. Guariglia, S. Silvestrov, Fractional-wavelet analysis of positive definite distributions and wavelets on $D'(C)$. in: *Engineering Mathematics II*, pp. 337–353. Springer, Berlin (2016)
56. S. Bankov, Antenna array with sequential excitation. *Litres* (2013)
57. T.A. Milligan, *Modern Antenna Design* (Wiley, New York, 2005)
58. D. Jackson, A. Oliner, BLeaky-wave antennas, in *Modern Antenna Handbook*, C. Balanis, Ed. New York: Wiley (2008)
59. Y. Sedelnikov, M. Shaaban, Ku band antenna for perspective telecommunication facilities. in: 2018 International Conference on Innovative Trends in Computer Engineering (ITCE), pp. 190–192 (2018). IEEE

60. Y. Li, C. Wang, Y.X. Guo, A ka-band wideband dual-polarized magnetoelectric dipole antenna array on Itcc. *IEEE Trans. Antennas Propag.* **68**(6), 4985–4990 (2019)
61. M. Ferrando-Rocher, J.I. Herranz-Herruzo, A. Valero-Nogueira, B. Bernardo-Clemente, A.U. Zaman, J. Yang, 8 × 8 ka-band dual-polarized array antenna based on gap waveguide technology. *IEEE Trans. Antennas Propag.* **67**(7), 4579–4588 (2019). <https://doi.org/10.1109/TAP.2019.2908109>
62. S.M. Sifat, M.M.M. Ali, S.I. Shams, A.-R. Sebak, High gain bow-tie slot antenna array loaded with grooves based on printed ridge gap waveguide technology. *IEEE Access* **7**, 36177–36185 (2019)
63. Z. Talepour, A. Khaleghi, Groove gap cavity slot array antenna for millimeter wave applications. *IEEE Trans. Antennas Propag.* **67**(1), 659–664 (2018). <https://doi.org/10.1109/TAP.2018.2879831>

Publisher's note

Springer Nature remains neutral with regard to jurisdictional claims in published maps and institutional affiliations.

Submit your manuscript to a SpringerOpen[®] journal and benefit from:

- Convenient online submission
- Rigorous peer review
- Open access: articles freely available online
- High visibility within the field
- Retaining the copyright to your article

Submit your next manuscript at ► [springeropen.com](https://www.springeropen.com)
